



UNIVERSITÀ  
DEGLI STUDI  
FIRENZE

# FLORE

## Repository istituzionale dell'Università degli Studi di Firenze

### **An Innovative Single Shot Power Quality Disturbance Detector Algorithm**

Questa è la Versione finale referata (Post print/Accepted manuscript) della seguente pubblicazione:

*Original Citation:*

An Innovative Single Shot Power Quality Disturbance Detector Algorithm / Iturrino-Garcia, C; Patrizi, G; Bartolini, A; Ciani, L; Paolucci, L; Luchetta, A; Grasso, F. - In: IEEE TRANSACTIONS ON INSTRUMENTATION AND MEASUREMENT. - ISSN 0018-9456. - ELETTRONICO. - 71:(2022), pp. 2517210.1-2517210.10. [10.1109/TIM.2022.3201927]

*Availability:*

The webpage <https://hdl.handle.net/2158/1283047> of the repository was last updated on 2022-11-07T10:57:30Z

*Published version:*

DOI: 10.1109/TIM.2022.3201927

*Terms of use:*

Open Access

La pubblicazione è resa disponibile sotto le norme e i termini della licenza di deposito, secondo quanto stabilito dalla Policy per l'accesso aperto dell'Università degli Studi di Firenze (<https://www.sba.unifi.it/upload/policy-oa-2016-1.pdf>)

*Publisher copyright claim:*

La data sopra indicata si riferisce all'ultimo aggiornamento della scheda del Repository FloRe - The above-mentioned date refers to the last update of the record in the Institutional Repository FloRe

(Article begins on next page)

# An Innovative Single Shot Power Quality Disturbance Detector Algorithm

Carlos Iturrino-García<sup>1</sup>, Gabriele Patrizi<sup>2</sup>, *Member, IEEE*, Alessandro Bartolini<sup>3</sup>, *Member, IEEE*, Lorenzo Ciani<sup>4</sup>, *Senior Member, IEEE*, Libero Paolucci<sup>5</sup>, Antonio Luchetta<sup>6</sup>, *Member, IEEE*, and Francesco Grasso<sup>7</sup>, *Member, IEEE*

**Abstract**—Power quality disturbances (PQDs) have affected many people due to the growing number of electronic nonlinear loads and because of the significant increase of renewable sources connected to the grid. Previous works have shown the development of algorithms to detect and classify these disturbances. A thorough review of PQD detector algorithms pointed out the use of machine learning and deep learning algorithms as the most used, accurate and up-to-date approaches to deal with this problem. Up until now, these algorithms were used in a sliding window manner that often fail to identify more than one disturbance in a single window frame. In this work, an innovative architecture called single shot PQD detection (SSPQDD) has been developed to solve this problem. Several experiments were conducted using a simulation dataset to validate the performances of the proposed SSPQDD in comparison with other algorithms available in literature in terms of computational resources, accuracy of identification, and number of layers. Furthermore, an experimental testbench has been carried out to test the performances of SSPQDD using real measurement data in case of multiple disturbances in a single window frame. The overall accuracy obtained using the proposed SSPQDD was 96.55% in PQD detection.

**Index Terms**—Artificial intelligence, neural networks (NNs), power distribution, power quality (PQ), smart grids.

## I. INTRODUCTION

**I**DEALLY, grid voltages and currents should have a purely sinusoidal waveform, but in reality they come in a distorted manner. These distortions vary in form and can have multiple sources that can affect multiple users in a community. These can be caused by the use of nonlinear electronic loads or by the generation of power by means of renewable sources.

Recently, renewable energy sources have engrossed great tendency because of their potential to solve problems like increasing the need for electrical power, decreasing air pollution, and tackling the problem of global warming. Wind energy and solar photovoltaic energy, among other sources, are more and more employed forming the hybrid power system network able to provide future energy demand. The intrinsic properties of these renewable sources (i.e., wind variations

and solar insolation changes) have a significant influence on power quality (PQ), reliability, and safety. As a result, low PQ levels could lead to motor failure, overheating of the lines, inaccurate metering, premature aging of devices, and disturbances in communication circuits [1], [2], [3]. Other than renewable energy sources, PQ problems can arise from the use of electronic devices and appliances that bring severe problems to grid voltages and currents in the form of PQ disturbances (PQDs).

In recent years, a large number of nonlinear loads and distributed generations with random characteristics have been connected to the power grid [4]. Although their extensive use in industrial, household, commercial, and public sectors have improved many aspects of everyday life, they have brought negative effects on the power grid. The use of nonlinear electronic loads has increased the eventuality of unbalanced currents, unacceptable harmonic levels, and poor power factor in three-phase distribution systems [5], [6]. In other words, power electronics technologies and/or nonlinear loads have made life easier and more comfortable but due to their nonlinear behavior it disturbs the power grid through voltage and current waveform distortions. As a consequence, to the extensive use of nonlinear electronic devices, the purely sinusoidal waveform gets injected with distorting components in an increasing rate which have degraded PQ levels. If distorting components are injected, power losses and malfunctioning of electric devices can occur. Common effects of a degradation of PQ in the industrial sector include loss of production, manufacturing interruption, loss of revenue, productivity cost, decrease competitiveness, lost opportunity, wasted energy, and the decrease of equipment life [7]. Similar effects can occur in the residential sector as overheating of ac appliances, television (TV) screens displaying flicker and data loss, malfunctioning communication equipment, and computer failures [8], [9]. Nonlinear electronic loads can also cause disturbance to other consumers and interference in nearby communication networks [10].

PQ is defined by the IEEE as “The concept of powering and grounding sensitive equipment in a manner that is suitable to the operation of that equipment” [11]. Any deviation, in voltage and current, from its nominal values in a certain period of time is considered a PQD. PQDs are classified as a deviation from its nominal magnitude and/or frequency components for a certain duration in time. According to IEEE Standard 1159-2009 (Recommended Practice for Moni-

Manuscript received 11 May 2022; revised 28 July 2022; accepted 19 August 2022. Date of publication 26 August 2022; date of current version 13 September 2022. The Associate Editor coordinating the review process was Zhenbing Zhao. (*Corresponding author: Lorenzo Ciani.*)

The authors are with the Department of Information Engineering, University of Florence, 50139 Florence, Italy (e-mail: carlos.iturrinogarcia@unifi.it; gabriele.patrizi@unifi.it; a.bartolini@unifi.it; lorenzo.ciani@unifi.it; libero.paolucci@unifi.it; antonio.luchetta@unifi.it; francesco.grasso@unifi.it).

Digital Object Identifier 10.1109/TIM.2022.3201927

toring Electric Power Quality) [12], the most common PQDs are as follows.

- 1) Transients (also known as surge) which could be classified as impulsive (with different time durations, from few ns up to over 1 ms) or oscillatory (i.e., low, medium and high frequency transients).
- 2) Short-duration root mean square (RMS) variations, such as sag, swell, interruption, and voltage imbalance which could be classified as instantaneous (from 10 to 600 ms), momentary (up to 3 s), and temporary (up to 1 min).
- 3) Long-duration RMS variations which include sustained interruption, undervoltage or overvoltage phenomenon, and current overload with typical duration longer than 1 min.
- 4) Wave distortions such as notch and harmonics.

Due to the problems that involve PQDs and the negative effects these may lead, it is important to detect and classify these disturbances. However, due to the very different nature of each PQD (in terms of duration, spectral content, magnitude, etc.), it is really challenging to develop an effective and efficient tool able to classify different categories of disturbances. For instance, Fare clic o toccare qui per immettere il testo. Urbina-Salas *et al.* [13] use the Wavelet and Hilbert transforms to instantaneously estimate several PQ indices, while in [14] the latter are evaluated using a set of new scaling filter and wavelet filter with narrow transition bands. Despite a good accuracy of the estimation, the approach presented in [14] is limited only to interharmonics and transient disturbances. Other approaches are able to solve this issue and classify properly different types of PQD using for instance time-dependent spectral features [15], sparse signal decomposition [16], and double resolution S-transform [17]. An extensive attempt has been made in previous works to detect and classify PQDs which many involve the use of machine learning (ML) and deep learning (DL) algorithms (see for instance but not only [18], [19], and [20]). Among the extensive inventory of ML and DL algorithms used to solve this problem, one of the most common and valid alternatives involves the use of convolutional neural networks (CNN) [21]. A CNN is a well-known DL architecture inspired by the natural visual perception mechanism of the living creatures [22], [23]. The extensive implementation of CNN arises from its feature extraction capabilities using convolutional operations within convolutional layers, and from the dimensionality reduction achieved using pooling layers. For instance, Shen *et al.* [24] integrates improved principal component analysis (IPCA) and a 1-D CNN to classify 12 types of synthetic and simulated PQDs. Instead, Wang and Chen [25] present a 1-D CNN to capture multiscale features and reduce overfitting extracting features from massive disturbance samples automatically. The problem with the majority of the approaches currently available in literature is that they move in a sliding window manner and use a conventional multiclass classification method. Thus, the current state-of-the-art is able to identify and classify only one PQD in a single window. This consideration led to the use

of very small sliding windows, with a consequent increase of computational complexity.

Recent advancement has been made for images using object detection algorithms. Among these algorithms the most famous are the you only look once (YOLO) [26] and the single shot detector (SSD) [27]. These algorithms were designed to identify and classify multiple objects in a single image. As images, voltage signals can contain multiple disturbances in a single window frame. If this type of signal is classified by a conventional method, it can lead to a misclassification. As a matter of fact, almost none of the approaches currently available in literature is able to correctly identify more than one disturbance in a single window. Trying to fill this gap, a new architecture for detection and classification of PQDs has been developed in this work integrating features from YOLO and SSD. The proposed deep learning architecture called single shot PQD detector (SSPQDD) is able to precisely identify the presence of a PQD and to accurately classify the disturbance type.

The major contributions of the proposed SSPQDD are described in the following.

- 1) Most of the approaches for PQ disturbance detection available in literature deals with threshold classification method based on the root mean square value of the acquired signal. Instead, the approach proposed in this research works with the entire voltage signal acquired by a dedicated instrument.
- 2) The proposed approach is not only able to identify the presence or not of a PQD, but it could also provide the duration of the disturbance.
- 3) The most important feature of the proposed method is the ability to precisely and accurately identify the presence of more than one disturbance in a single sliding window with a number of parameters, a number of layers, and a computational complexity lower than the other approaches for image classification available in literature.

The rest of the article is organized as follows: Section II introduce the proposed SSPQDD algorithm, Section III illustrates the results obtained using a simulated dataset and a comparison with other approaches available in literature, while Section IV shows the results obtained analyzing the PQ measurement obtained using a smart PQ meter provided by PowerEmp Srl.

## II. PROPOSED APPROACH

### A. Architecture

The proposed SSPQDD is based on a pretrained VGG-16 architecture. The VGG-16 is a deep CNN proposed by Simonyan and Zisserman from the University of Oxford in 2014. In the last years, VGG16 has been used for image recognition or classification and for image detection and localization, while it is not used for PQD classification. In this work, the base architecture of the proposed SSPQDD is a VGG-16 network because of its outstanding accuracy in classifying PQDs compared to other architectures presented in this work. The results of this comparison are shown in Section III.

**Algorithm 1** Proposed SSPQDD Method.  $\alpha = 0.00005$ ,  $\beta_1 = 0.5$ ,  $\beta_2 = 0.999$ ,  $N = 6$ , and  $G = 188$ 

**Require:** Input  $x$ , target class  $y_{class}$ , target confidence  $y_{conf}$ , number of classes  $N$ , number of grids  $G$ , training mask  $M_{St}$ , batch size  $m$ , and Adam hyperparameters  $\alpha$ ,  $\beta_1$ , and  $\beta_2$ .

```

1: while  $\theta$  has not converged do:
2:   Sample data batch  $\{x^{(1)}, \dots, x^{(m)}\}$  from dataset  $x \sim P_{data}$ 
3:   Sample target batch  $\{y_{class}^{(1)}, \dots, y_{class}^{(m)}\}$  and  $\{y_{conf}^{(1)}, \dots, y_{conf}^{(m)}\}$  from  $y_{class} \sim P_{class}$  and  $y_{conf} \sim P_{conf}$ 
4:   for  $i = 1 \dots m$  do:
5:      $St_{class}(x^{(i)}) \leftarrow softmax(class(x^{(i)})) \circ M_{St}$ 
6:      $St_{conf}(x^{(i)}) \leftarrow softmax(conf(x^{(i)}))$ 
7:      $L^{(i)} = - \sum_{g=1}^G \left[ \sum_{t=1}^N \left[ y_{class(t,g)}^{(i)} \log[St_{class}(x^{(i)})_{(t,g)}] \right] + y_{conf_g}^{(i)} \log[St_{conf_g}(x^{(i)})] + (1 - y_{conf_g}^{(i)}) \log[1 - St_{conf_g}(x^{(i)})] \right]$ 
8:   end for
9:    $\theta \leftarrow Adam(\nabla_{\theta} \frac{1}{m} \sum_{i=1}^m L^{(i)}, \theta, \alpha, \beta_1, \beta_2)$ 
10: end while

```

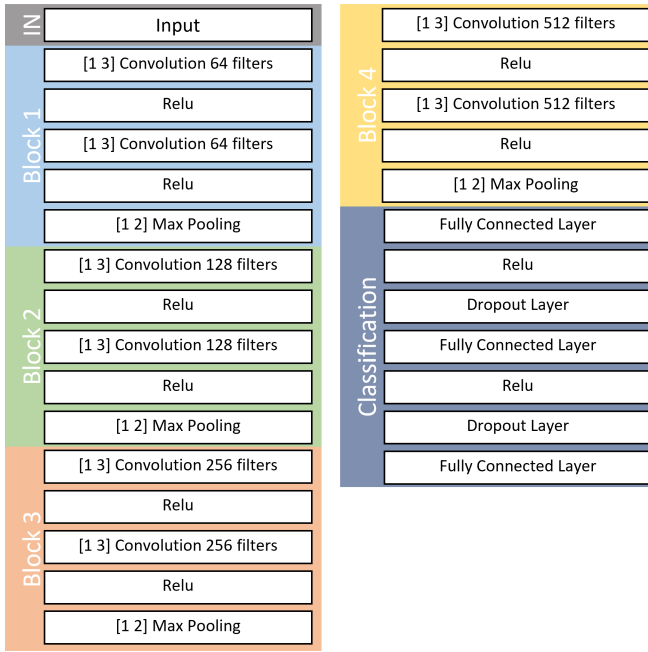


Fig. 1. Architecture of the base VGG-16 network used in this work.

After the training of the base network, the fully connected layers are substituted by feature extraction layers. This is done to take advantage of the maxpooling layers typical of the VGG-16 architecture and to classify voltage signals in a grid like structure. The proposed approach classifies 16 samples of the voltage signal per grid. Fig. 1 shows the VGG-16 base architecture, which is divided into six consecutive blocks (each one is identified using a different background color in the figure). The first block is the input and the following blocks are the convolutional blocks where the kernel size are  $1 \times 3$  arrays. In block 1, the filter size is 64 and increments by a factor of 2 for each size being 512 in the last block. Finally, the last block is the classification layer which contains 4096 layers for each fully connected layer. For generalization purposes, a dropout layer is added with 50% dropout.

Fig. 2 shows the block diagram of the proposed method in which the base network is the VGG16 architecture, and the feedforward layers are substituted by feature extraction layers for the grid-like classification. The added stage uses a maxpooling layer for dimensionality reduction or, in other

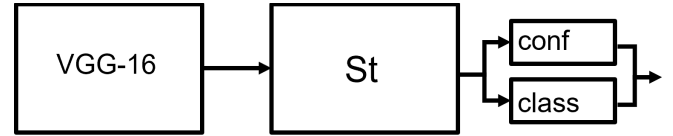


Fig. 2. Schematic representation of the proposed SSPQDD architecture.

words, for classification of a larger number of samples. The final layer has two outputs. The first output, the confidence output, is a binary classification that classifies the signal as disturbance or no disturbance. The confidence output is used to mask the second output which is a multiclass classification. St has 188 grids which are 16 samples per grid. This is fundamental to ensure that the algorithm will be able to find and classify transient disturbances of few nanoseconds as well as temporary disturbances lasting over 1 min.

The confidence output is characterized by two outputs per grid, while the classification one has six output per grid due to the six types of disturbances taken into consideration. These include sag, swell, harmonic, transient, notch, and interruption. A confidence of class 0 means normal.

### B. Dataset

The dataset used to train and validate the proposed network involves voltage signals containing sag, swell, harmonics, transient, notch, and interruption. All the PQDs have been generated randomly within the signal to ensure different time durations of the disturbances and to cover different locations in a window frame. The dataset was generated using MATLAB Simulink considering a sampling frequency of 8 kHz for a total duration of 3.75 s. A 3.75 s sliding window have been selected since it represents the greatest window that could be implemented on the available hardware considering a 8 kHz sampling frequency. The limit on the window dimension is due only to the computational complexity required by the hardware device and it does not affect the classification accuracy.

The dimension of the training dataset was 290 MB and the time required to train the proposed network was approximately one day. However, this could not be considered a limitation since training is required only once, before the first use of the SSPQDD algorithm.

The target includes the confidence matrices and the classification matrices. The classification matrices are multiplied



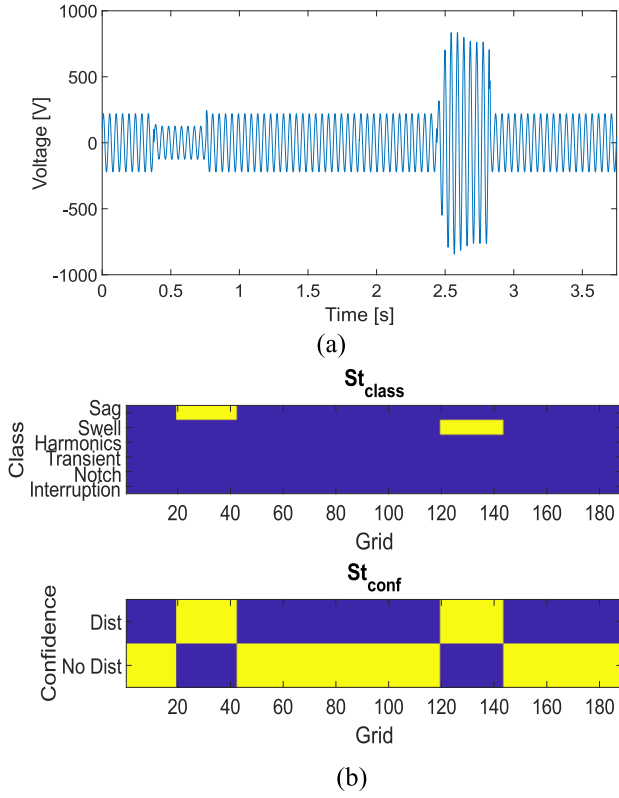


Fig. 3. Illustration of the training phase for the proposed algorithm. (a) Voltage signal containing a swell and a sag. (b). Classification and Confidence matrices in the  $St$  layer.

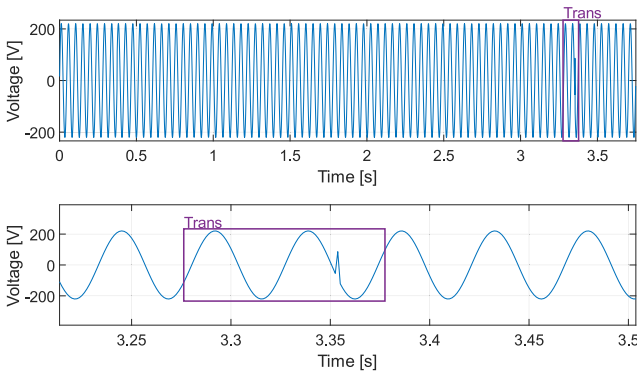


Fig. 4. Results obtained in case of a transient disturbance in the simulated dataset.

by a mask matrix for training stability purposes. The matrices are  $2 \times 188$  for the confidence matrices and  $6 \times 188$  for the classification matrices. The output is then confronted with the confidence and classification matrices.

Fig. 3(a) shows an extract of the voltage signal used to train the algorithm including a swell disturbance instantaneously followed by a sag disturbance. Below the voltage signal there are the training matrices shown in Fig. 3(b) representing the classification matrices and the confidence matrices.

Pretraining of the VGG16 is done classifying the disturbance as a multiclass classification problem using the softmax function. The fully connected layers are then removed, and the

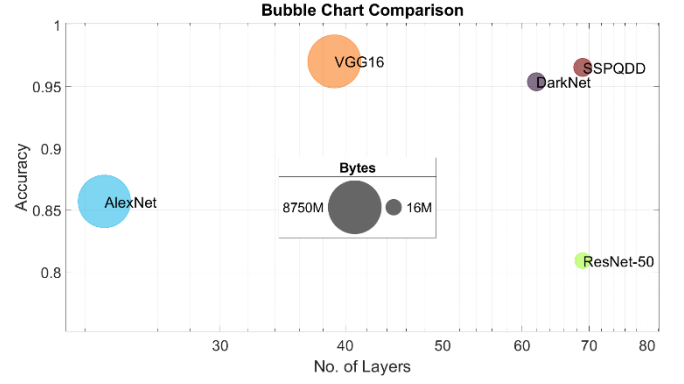


Fig. 5. Comparative analysis results: accuracy, number of layers, and computational complexity (in terms of required memory) of the proposed SSPQDD method against other CNN-based approaches.

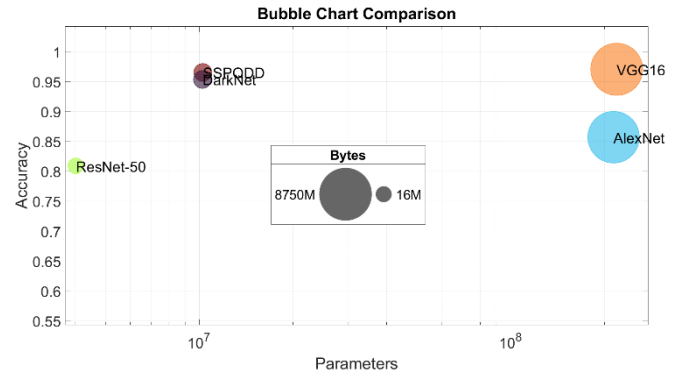


Fig. 6. Comparative analysis results: accuracy, number of parameters, and computational complexity (in terms of required memory) of the proposed SSPQDD method against other CNN-based approaches.

feature extraction layers and the output layers are then added to the base network. Training of the SSPQDD network is done with voltage signals and comparing the outputs with the target matrices shown in Fig. 3(b). The softmax function is used in a binary manner on each grid to determine if a PQD exists in that given grid. Thus, the probability to classify the  $j$ th class given a sample vector  $x$  and  $a$  weighting vector  $w$  is given by

$$P(\hat{y} = j | x) = \frac{e^{x^T w_j}}{\sum_{l=1}^K e^{x^T w_l}}. \quad (1)$$

The multiclass softmax function is used in the classification output. The classification output, after the softmax, is then multiplied by a mask matrix for training stability purposes and class imbalances. The loss function is then calculated using the crossentropy loss. The crossentropy loss and the binary crossentropy loss are shown in (2) and (3), respectively.

The  $y_{conf}$  and  $y_{class}$  are the target matrices for the confidence output and the class output, respectively. The  $St_{\eta_{conf}}(x)_t$  and the  $St_{\eta_{class}}(x)_t$  are the outputs of the confidence and the class of the proposed SSPQDD architecture.

From the available dataset the input  $x$  can be extracted (i.e., the signal to be classified). The target class  $y_{class}$  and the target confidence  $y_{conf}$  are the matrices that are compared with the output. The  $N$  and  $G$  are the number of classes and the number of grids, respectively.  $M_{St}$  is the training mask that is the first

TABLE I  
COMPARISON OF DEEP LEARNING ARCHITECTURES FOR PQD CLASSIFICATION

GOODNESS METRIC	NORMAL	SAG	SWELL	HARMONICS	TRANSIENT	NOTCH	INTERRUPTION
<b>DarkNet Architecture</b>							
Precision	83.0%	99.4%	99.5%	97.5%	93.1%	93.9%	96.2%
Recall	100%	100%	96.5%	88.2%	75.5%	99.6%	100%
F1-Score	90.7%	99.7%	98.0%	92.6%	83.4%	96.7%	98.1%
AUC	0.985	1	0.982	0.941	0.941	0.998	0.998
<b>AlexNet architecture</b>							
Precision	0%	99.9%	100%	100%	49.8%	100%	100%
Recall	0%	100%	100%	100%	100%	100%	99.9%
F1-Score	0%	99.95%	100%	100%	66.48%	100%	100%
AUC	0.5	0.999	1	1	0.913	1	1
<b>ResNet Architecture</b>							
Precision	0%	100%	100%	100%	42.7%	100%	100%
Recall	0%	100%	99.0%	79.5%	100%	100%	87.8%
F1-Score	0%	100%	99.49%	88.57%	59.85%	100%	93.5%
AUC	0.5	1	0.995	0.898	0.887	1	0.939
<b>Basic VGG-16 architecture</b>							
Precision	94.5%	99.5%	97.8%	99.7%	96.7%	93.6%	97.9%
Recall	99.8%	97.6%	98.9%	99.1%	85.8%	98.1%	100%
F1-Score	97.08%	98.54%	98.35%	99.4%	90.92%	95.8%	98.94%
AUC	0.994	0.9847	0.992	99.6	0.927	0.981	0.999
<b>Proposed SSPQDD architecture</b>							
Precision	83.2%	100%	100%	100%	100%	100%	100%
Recall	100%	100%	100%	100%	79.7%	100%	100%
F1-Score	90.82%	100%	100%	100%	88.7%	100%	100%
AUC	0.984	1	1	1	0.899	1	1

row of  $y_{\text{conf}}$ . The training parameters are the batch size  $m$  and the Adaptive Moment Optimizer (Adam) hyperparameters  $\alpha$ ,  $\beta_1$ , and  $\beta_2$

$$\begin{aligned}
 & - \sum_{t=1}^N y_{\text{class}_t} \log[\text{St}_{\eta_{\text{class}}}(x)_t] \\
 & \sum_{t=1}^N [y_{\text{conf}_t} \log[\text{St}_{\eta_{\text{conf}}}(x)_t] + (1 - y_{\text{conf}_t}) \log[1 - \text{St}_{\eta_{\text{conf}}}(x)_t]].
 \end{aligned} \quad (2)$$

The loss of the confidence and of the classifications are then added and the weights of the proposed network are updated using the Adam algorithm. The complete algorithm of the proposed SSPQDD is shown in Algorithm 1. After the algorithm is tested, the confidence matrices are then multiplied to the classification matrices to find the disturbance in the signal frame as show in (4) and (5). The  $\text{St}_{\eta_{\text{class}}}$  is a  $N \times G$  matrix with each class represented by  $N$  and each grid represented by  $G$ .  $\text{St}_{\eta_{\text{class}}}$  is the softmax of each grid multiplied

by the first row of the confidence

$$\begin{aligned}
 & H[n, g] \\
 & = \text{softmax}(\text{class}(x)[g]) \\
 & \text{St}_{\eta_{\text{class}}} \\
 & = \begin{bmatrix} H[1, 1] * \text{St}_{\eta_{\text{conf}}}[1, 1] & \cdots & H[1, G] * \text{St}_{\eta_{\text{conf}}}[1, G] \\ \vdots & \ddots & \vdots \\ H[N, 1] * \text{St}_{\eta_{\text{conf}}}[1, 1] & \cdots & H[N, G] * \text{St}_{\eta_{\text{conf}}}[1, G] \end{bmatrix}.
 \end{aligned} \quad (4)$$

An example of PQD classification performed using the proposed SSPQDD architecture is illustrated in Fig. 4, where the output of the network in case of a transient disturbance is illustrated. The top subplot shows how, using the proposed architecture, even a small sliding window is able to identify the transient.

### III. COMPARATIVE ANALYSIS WITH OTHER DEEP LEARNING APPROACHES AVAILABLE IN LITERATURE

In this section, the proposed SSPQDD was compared to well-known deep learning architectures that show good results

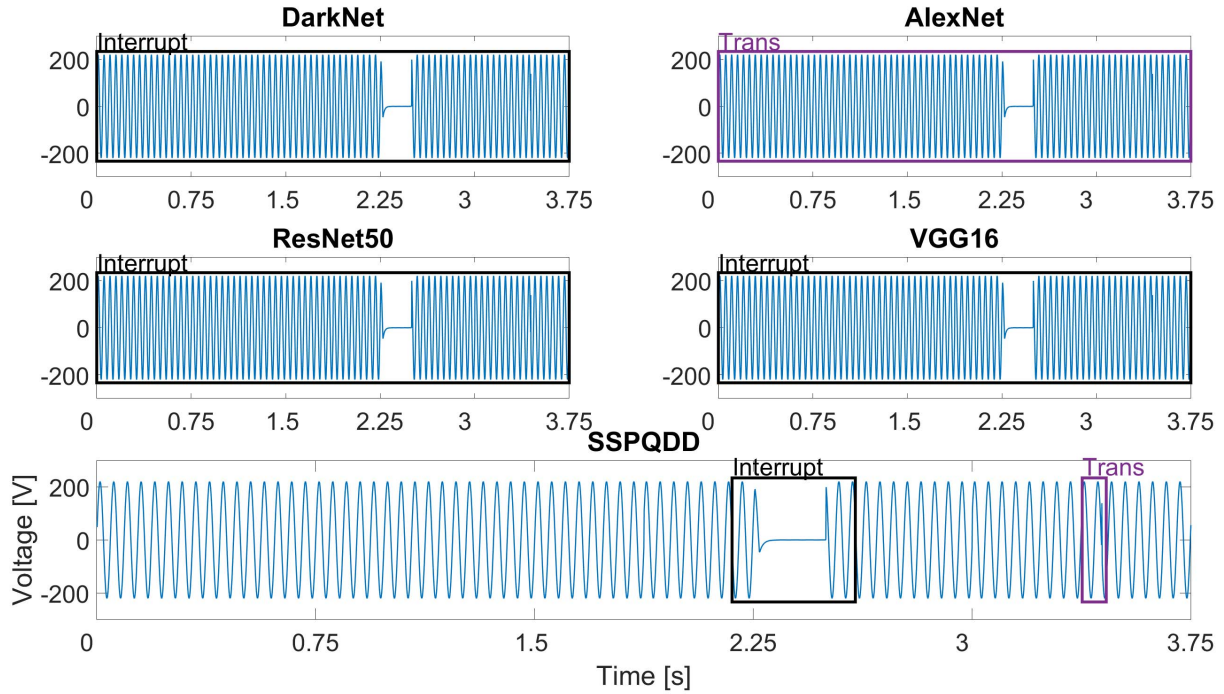


Fig. 7. Extract of the results obtained in PQD classification using the proposed SSPQDD network (bottom subplot) in the presence of two different disturbances (a first interruption followed by a transient). The top subplots refer to the other CNN-based approaches used as comparative analysis.

in image classification tasks. Currently, there are no methods available in literature that uses neural network (NN) specifically developed for PQD detection. Quite the contrary, there are few approaches that uses NN developed for image classification to tackle the problem exactly as an image classification problem (in each frame of the acquired signal the network looks for a PQD).

To compare these architectures, an experiment was made training all architectures and comparing their performances. Due to the nature of classification of the grid-like structured in early stages, the SSPQDD can detect disturbances in voltage signals that have duration from few nanoseconds up to over 1 min. The dataset used for training the different deep learning architecture was the same used for the SSPQDD, as described in the previous section. The architectures used to compare the performances of the proposed SSPQDD are the following.

- 1) DarkNet [28], which is a fast and simple deep learning-based object detection framework.
- 2) AlexNet [29], which is a milestone in deep CNN and it is based on eight layers (five convolutional layers and three fully connected layers).
- 3) ResNet [30] which is a significantly deep network implemented using layer skips.
- 4) The basic VGG16 network [31].

The results of the comparison are shown in Figs. 5 and 6. More in detail, the first comparison has been carried out measuring the accuracy, the number of layers, and the computational resources required for each architecture, as shown in Fig. 5. Similarly, Fig. 6 compares the accuracy of each architecture, taking into account also the number of network's parameters. The highest accuracy was obtained using the basic VGG16. However, the latter network requires a lot of computational effort due the considerably great number of

parameters, as it is possible to see analyzing the figures. Quite the contrary, the proposed SSPQDD architecture does not require that much of memory space, and it is capable of achieving remarkably high accuracy despite a substantially lower number of parameters.

Investigating more in detail the results obtained for every PQD under analysis, the different architectures show good results for each disturbance except for the transient and the normal condition. The VGG16 represents the exception since it is capable to found most of the transients even better than the proposed network. This is the reason why it has been chosen for the base network of the SSPQDD. The problem with the VGG16 is that it fails to identify where the disturbances are in the window frame.

Table I shows the precision, recall, F1-score and the area under the receiver operating characteristic (ROC) curve [also known as area under the ROC curve (AUC)] of the different architectures for each class of disturbance under consideration.

For the normal class or no disturbance DarkNet and ResNet gave a 0% result due to their limited capabilities differentiating the normal from the transient. Similarly, also the AlexNet resulted in 0% precision and 100% recall for the normal class.

On the other hand, the VGG16 and the SSPQDD resulted in high precision, recall, F1-score (i.e., the harmonic mean between precision and recall) and AUC for the normal class. Other than the normal class, each architecture gave good results, even if the VGG16 and the proposed SSPQDD network provide the highest accuracy and the better results for each analyzed class.

Overall, the VGG16 provide a total accuracy of 97.04% while the proposed network reaches the 96.55%.

Results using training data also highlight how the proposed SSPQDD represent the only available approach able to detect multiple disturbances with different durations and

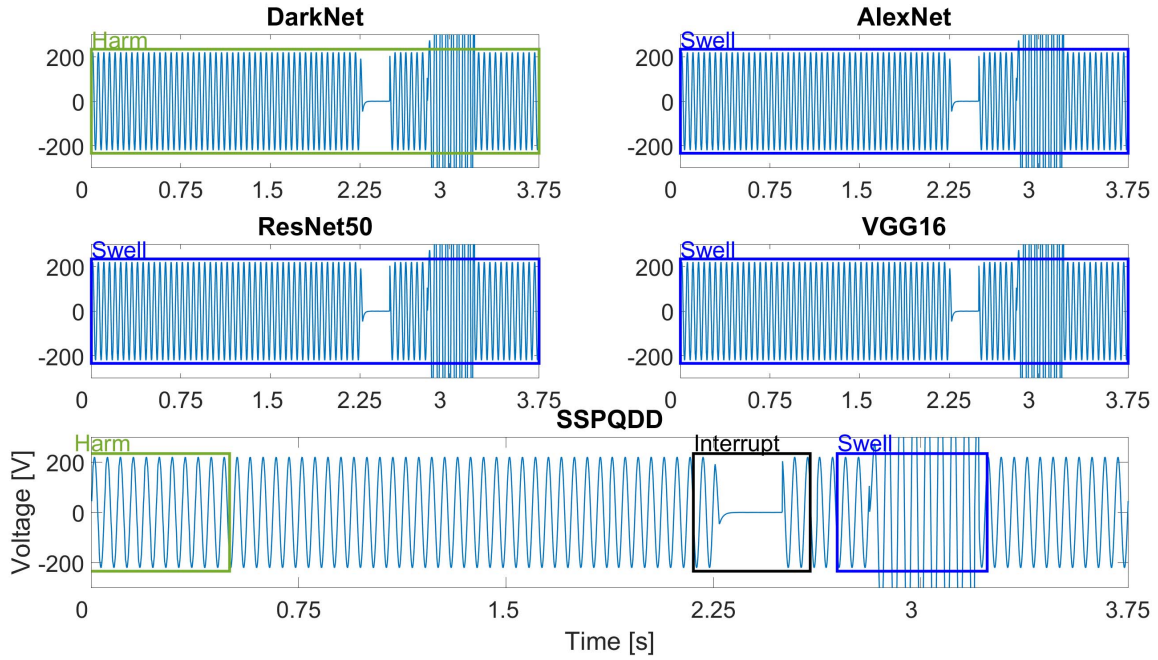


Fig. 8. Extract of the results obtained in PQD classification using the proposed SSPQDD network (bottom subplot) in presence of three different disturbances (an harmonic disturbance followed by an interruption and a swell). The top subplots refer to the other CNN-based approaches used as comparative analysis.

different locations in a single window frame. More in detail, Fig. 7 illustrates the results obtained using the simulated dataset in case of two disturbances of different kinds and different durations in the same window. The random signal illustrated in Fig. 7 includes an interruption of over 200 ms followed by a short transient less than a second later. The proposed architecture is the only one able to detect both PQDs, while DarkNet, resNet, and VGG-16 can detect only the first long Interruption. Quite the opposite, the AlexNet is able to detect only the interruption, completely missing the identification of the major long interruption. This is even more clear analyzing Fig. 8, where the random voltage signal includes three different disturbances: an harmonic followed by a long interruption and a swell. Also in this case, the proposed SSPQDD algorithm is the only one able to detect all the disturbance in a single window. The DarkNet identifies only the harmonics, while AlexNet, ResNet, and VGG-16 identify only the swell. This means that all the state-of-the-art networks used for comparison completely miss to identify a long interruption of over 200 ms, which is not acceptable in almost every application.

The analysis in Figs. 7 and 8 summarizes entirely the major contributions brought by the proposed algorithm and the research gap filled by the SSPQDD. Both figures highlight perfectly the most critical, powerful, and important feature of the approach, ensuring also levels of accuracy on the single disturbance comparable with the most outstanding works available in literature (as summarized in Table I).

#### IV. EXPERIMENTAL ANALYSIS

The final validation of the proposed SSPQDD algorithm has been carried out using an experimental measurement

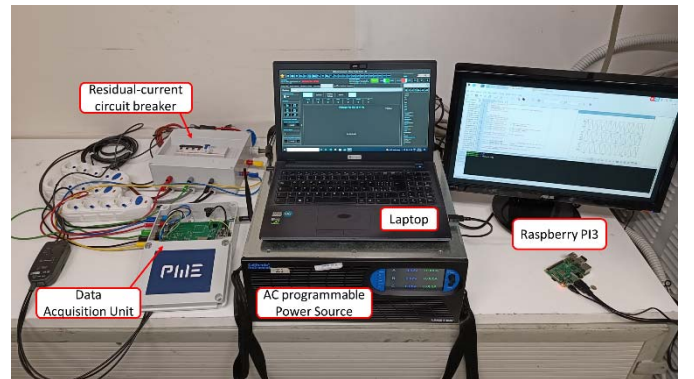


Fig. 9. Experimental setup used to test the performances of the proposed SSPQDD algorithm.

setup able to acquire voltage signals and process real-time classification algorithms to rapidly and precisely identify PQ disturbances.

A picture of the experimental setup is reported in Fig. 9, showing the ac programmable power source which could be controlled by a laptop to generate a three-phase power source affected by different disturbances.

A smart PQ meter provided by PowerEmp Srl has been used to analyze the electrical parameters of the power source and evaluate its health status. Furthermore, the PQ meter serves as data acquisition unit able to transmit the voltage signals acquired on each phase to a Raspberry PI 3b through a Wi-Fi protocol. The Raspberry PI 3b has been used to run the SSPQDD algorithm and classify the disturbances generated on the grid by the programmable power source.

The first thing to note is the possibility to run the SSPQDD algorithm on embedded electronics with limited computational resources like a Raspberry PI 3b. This is a fundamental aspect



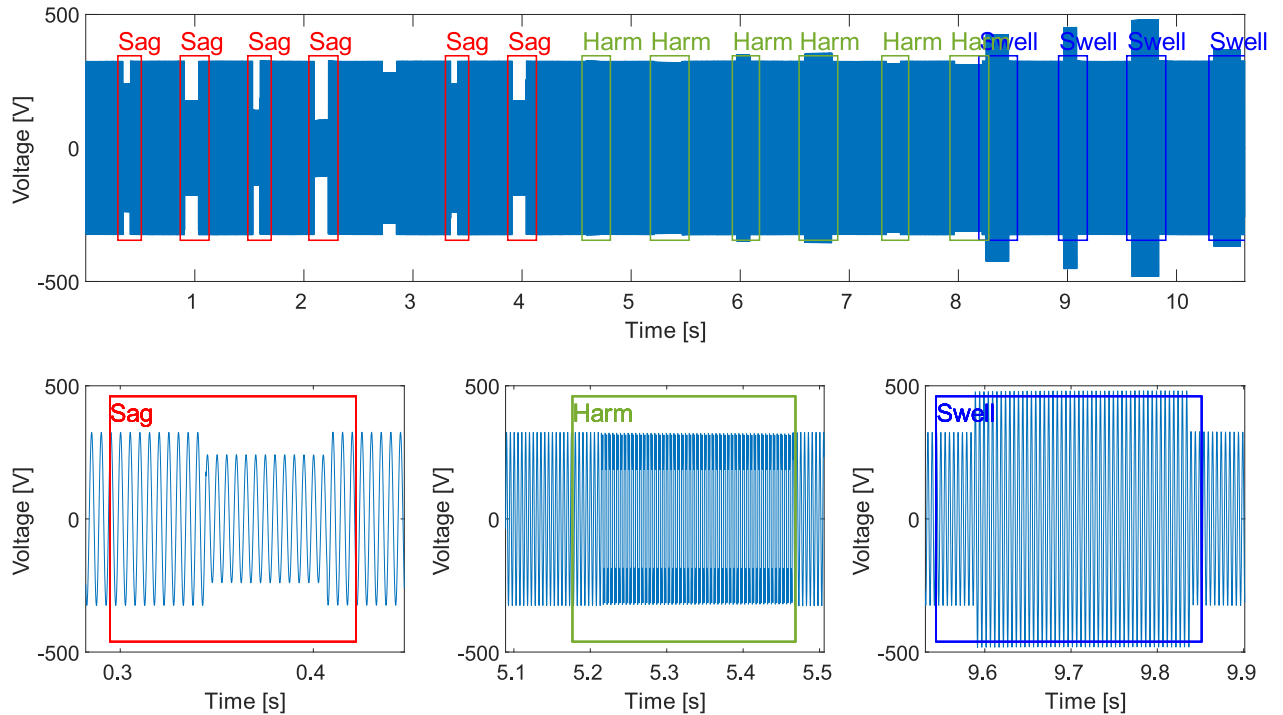


Fig. 10. Classification results obtained using the proposed SSPQDD analyzing the measurement acquisition in presence of multiple disturbances.

for the applicability ranges of the proposed method, which has proven to be one of the few alternatives allowing this option. A solution such as VGG-16 ensures slightly higher accuracy than the proposed method, but it could not be implemented on embedded electronics.

The disturbances that were generated using the experimental measurement setup included sag, swell, interruption, and harmonics. The measurement device sends real-time data to the Raspberry PI 3b, which automatically runs the algorithm on the acquired data and classifies the disturbance. At the same time, data were also sent to a computer to run post-processing algorithms such as DarkNet, AlexNet, ResNet, and VGG-16.

Once again, the SSPQDD has been able to detect and classify all the disturbances correctly, regardless the time duration, the location within the window frame and the number of disturbances within the same window. The results obtained in this scenario are illustrated in Fig. 10, identifying with different colors each disturbance classified by the proposed architecture. The top subplot in Fig. 10 shows a significant portion of the measured signal including 15 different disturbances, while the bottom subplots emphasize three different kinds of PQDs classified using smaller windows.

All the other approaches tested in the work missed to classify multiple disturbances, proving once again the potentiality of the proposed approach.

## V. CONCLUSION

This work deals with the classification of PQDs using a CNN-based approach. A simulated dataset of voltage signals containing different voltage disturbances has been generated using MATLAB Simulink to train the proposed SSPQDD

deep learning architecture. The training of the SSPQDD has been carried out following the guidelines presented in the proposed Algorithm 1. To test the effectiveness and the contributions of the proposed approach, the results obtained using the SSPQDD have been compared with classical deep learning architectures. The proposed SSPQDD has proven to be superior to the other approaches in almost all aspects (including accuracy, number of layers, computational complexity, and number of parameters). In fact, other than being superior in performances, the SSPQDD has proven to be efficient in terms of use of computational resources. This is due to the lack of feed forward network that usually requires most of the computational effort. With that been said, the SSPQDD can be an outstanding candidate for use in embedded electronics, where the amount of computational resources plays a significant role in the selection process of the DL architecture.

Experimental results prove that the SSPQDD can effectively and efficiently detect and classify multiple voltage disturbances in a single window frame. These disturbances varied in duration and intensity, and the SSPQDD detected and classified each one of them effectively. Quite the contrary, the other methods available in literature fail to classify more than one disturbance in a single window, missing to consider even long and major disturbances.

## ACKNOWLEDGMENT

The authors would like to express their sincere thanks to PowerEmp srl for providing the smart PQ meter used in the experimental measurement setup.

## REFERENCES

- [1] A. Akbarpour, M. Nafar, and M. Simab, "Multiple power quality disturbances detection and classification with fluctuations of amplitude and decision tree algorithm," *Electr. Eng.*, vol. 104, no. 4, pp. 2333–2343, Aug. 2022, doi: [10.1007/s00202-021-01481-5](https://doi.org/10.1007/s00202-021-01481-5).
- [2] G. Artale *et al.*, "Measurement of simplified single- and three-phase parameters for harmonic emission assessment based on IEEE 1459–2010," *IEEE Trans. Instrum. Meas.*, vol. 70, pp. 1–10, 2021, doi: [10.1109/TIM.2020.3037949](https://doi.org/10.1109/TIM.2020.3037949).
- [3] L. D. O. Arenas, G. de Azevedo e Melo, and C. A. Canesin, "A methodology for power quantities calculation applied to an FPGA-based smart-energy meter," *IEEE Trans. Instrum. Meas.*, vol. 70, pp. 1–11, 2021, doi: [10.1109/TIM.2020.3034978](https://doi.org/10.1109/TIM.2020.3034978).
- [4] Y. Zhang, Y. Zhang, and X. Zhou, "Classification of power quality disturbances using visual attention mechanism and feed-forward neural network," *Measurement*, vol. 188, Jan. 2022, Art. no. 110390, doi: [10.1016/j.measurement.2021.110390](https://doi.org/10.1016/j.measurement.2021.110390).
- [5] D. Sharon, J.-C. Montano, A. Lopez, M. Castilla, D. Borrás, and J. Gutierrez, "Power quality factor for networks supplying unbalanced nonlinear loads," *IEEE Trans. Instrum. Meas.*, vol. 57, no. 6, pp. 1268–1274, Jun. 2008, doi: [10.1109/TIM.2007.915146](https://doi.org/10.1109/TIM.2007.915146).
- [6] R. Kumar, B. Singh, R. Kumar, and S. Marwaha, "Recognition of underlying causes of power quality disturbances using stockwell transform," *IEEE Trans. Instrum. Meas.*, vol. 69, no. 6, pp. 2798–2807, Jun. 2020, doi: [10.1109/TIM.2019.2926876](https://doi.org/10.1109/TIM.2019.2926876).
- [7] M. I. Muhamad, N. Mariun, and M. A. M. Radzi, "The effects of power quality to the industries," in *Proc. 5th Student Conf. Res. Develop.*, 2007, pp. 1–4, doi: [10.1109/SCORED.2007.4451410](https://doi.org/10.1109/SCORED.2007.4451410).
- [8] R. S. Kumar, I. G. C. Raj, S. Saravanan, P. Leninpugalhanthi, and P. Pandiyan, "Impact of power quality issues in residential systems," in *Power Quality in Modern Power Systems*. Amsterdam, The Netherlands: Elsevier, 2021, pp. 163–191, doi: [10.1016/B978-0-12-823346-7.00009-8](https://doi.org/10.1016/B978-0-12-823346-7.00009-8).
- [9] F.-C. Argatu, V. Brezoianu, V. V. Argatu, B.-A. Enache, F.-C. Adochiei, and T. Icleanu, "Power quality analyzer for smart grid-smart home applications," in *Proc. 54th Int. Universities Power Eng. Conf. (UPEC)*, Sep. 2019, pp. 1–4, doi: [10.1109/UPEC.2019.8893501](https://doi.org/10.1109/UPEC.2019.8893501).
- [10] B. Singh, K. Al-Haddad, and A. Chandra, "A review of active filters for power quality improvement," *IEEE Trans. Ind. Electron.*, vol. 46, no. 5, pp. 960–971, Oct. 1999, doi: [10.1109/41.793345](https://doi.org/10.1109/41.793345).
- [11] G. Benysek, *Improvement in the Quality of Delivery of Electrical Energy using Power Electronics Systems*. London, U.K.: Springer, 2007.
- [12] IEEE Power and Energy Society, *IEEE Recommended Practice for Monitoring Electric Power Quality*, Standard 1159–2009, 2009, doi: [10.1109/IEEESTD.2009.5154067](https://doi.org/10.1109/IEEESTD.2009.5154067).
- [13] I. Urbina-Salas, J. R. Razo-Hernandez, D. Granados-Lieberman, M. Valtierra-Rodriguez, and J. E. Torres-Fernandez, "Instantaneous power quality indices based on single-sideband modulation and wavelet packet-Hilbert transform," *IEEE Trans. Instrum. Meas.*, vol. 66, no. 5, pp. 1021–1031, May 2017, doi: [10.1109/TIM.2017.2663560](https://doi.org/10.1109/TIM.2017.2663560).
- [14] Y. Yu, W. Zhao, S. Li, and S. Huang, "A two-stage wavelet decomposition method for instantaneous power quality indices estimation considering interharmonics and transient disturbances," *IEEE Trans. Instrum. Meas.*, vol. 70, pp. 1–13, 2021, doi: [10.1109/TIM.2021.3052554](https://doi.org/10.1109/TIM.2021.3052554).
- [15] Y. Liu, T. Jin, M. A. Mohamed, and Q. Wang, "A novel three-step classification approach based on time-dependent spectral features for complex power quality disturbances," *IEEE Trans. Instrum. Meas.*, vol. 70, pp. 1–14, 2021, doi: [10.1109/TIM.2021.3050187](https://doi.org/10.1109/TIM.2021.3050187).
- [16] M. S. Manikandan, S. R. Samantaray, and I. Kamwa, "Detection and classification of power quality disturbances using sparse signal decomposition on hybrid dictionaries," *IEEE Trans. Instrum. Meas.*, vol. 64, no. 1, pp. 27–38, Jan. 2015, doi: [10.1109/TIM.2014.2330493](https://doi.org/10.1109/TIM.2014.2330493).
- [17] J. Li, Z. Teng, Q. Tang, and J. Song, "Detection and classification of power quality disturbances using double resolution S-transform and DAG-SVMs," *IEEE Trans. Instrum. Meas.*, vol. 65, no. 10, pp. 2302–2312, Oct. 2016, doi: [10.1109/TIM.2016.2578518](https://doi.org/10.1109/TIM.2016.2578518).
- [18] N. Mohan, K. P. Soman, and R. Vinayakumar, "Deep power: Deep learning architectures for power quality disturbances classification," in *Proc. Int. Conf. Technol. Advancements Power Energy (TAP Energy)*, Dec. 2017, pp. 1–6, doi: [10.1109/TAPENERGY.2017.8397249](https://doi.org/10.1109/TAPENERGY.2017.8397249).
- [19] C. I. Garcia, F. Grasso, A. Luchetta, M. C. Piccirilli, L. Paolucci, and G. Talluri, "A comparison of power quality disturbance detection and classification methods using CNN, LSTM and CNN-LSTM," *Appl. Sci.*, vol. 10, no. 19, p. 6755, Sep. 2020, doi: [10.3390/app10196755](https://doi.org/10.3390/app10196755).
- [20] M. Shafiullah, M. A. M. Khan, and S. D. Ahmed, "PQ disturbance detection and classification combining advanced signal processing and machine learning tools," in *Power Quality in Modern Power Systems*. Amsterdam, The Netherlands: Elsevier, 2021, pp. 311–335, doi: [10.1016/B978-0-12-823346-7.00012-8](https://doi.org/10.1016/B978-0-12-823346-7.00012-8).
- [21] H. Xue, A. Chen, D. Zhang, and C. Zhang, "A novel deep convolution neural network and spectrogram based microgrid power quality disturbances classification method," in *Proc. IEEE Appl. Power Electron. Conf. Expo. (APEC)*, Mar. 2020, pp. 2303–2307, doi: [10.1109/APEC39645.2020.9124252](https://doi.org/10.1109/APEC39645.2020.9124252).
- [22] J. Gu *et al.*, "Recent advances in convolutional neural networks," *Pattern Recognit.*, vol. 77, pp. 354–377, May 2018, doi: [10.1016/j.patcog.2017.10.013](https://doi.org/10.1016/j.patcog.2017.10.013).
- [23] X. Jiang and Z. Ge, "Augmented multidimensional convolutional neural network for industrial soft sensing," *IEEE Trans. Instrum. Meas.*, vol. 70, pp. 1–10, 2021, doi: [10.1109/TIM.2021.3075515](https://doi.org/10.1109/TIM.2021.3075515).
- [24] Y. Shen, M. Abubakar, H. Liu, and F. Hussain, "Power quality disturbance monitoring and classification based on improved PCA and convolution neural network for wind-grid distribution systems," *Energies*, vol. 12, no. 7, p. 1280, Apr. 2019, doi: [10.3390/en12071280](https://doi.org/10.3390/en12071280).
- [25] S. Wang and H. Chen, "A novel deep learning method for the classification of power quality disturbances using deep convolutional neural network," *Appl. Energy*, vol. 235, pp. 1126–1140, Feb. 2019, doi: [10.1016/j.apenergy.2018.09.160](https://doi.org/10.1016/j.apenergy.2018.09.160).
- [26] J. Redmon, S. Divvala, R. Girshick, and A. Farhadi, "You only look once: Unified, real-time object detection," in *Proc. IEEE Conf. Comput. Vis. Pattern Recognit. (CVPR)*, Jun. 2016, pp. 779–788, doi: [10.1109/CVPR.2016.91](https://doi.org/10.1109/CVPR.2016.91).
- [27] W. Liu *et al.*, "SSD: Single shot MultiBox detector," in *Proc. Eur. Conf. Comput. Vis. (ECCV)*, Amsterdam, The Netherlands, Oct. 2016.
- [28] J. Redmon. *DarkNet*. Accessed: Apr. 27, 2022. [Online]. Available: <https://github.com/pjreddie/darknet>
- [29] A. Krizhevsky, I. Sutskever, and G. E. Hinton, "Imagenet classification with deep convolutional neural networks," in *Proc. 26th Annu. Conf. Neural Inf. Process. Syst. Lake Tahoe, NV, USA*, vol. 2, Dec. 2012, pp. 1097–1105.
- [30] K. He, X. Zhang, S. Ren, and J. Sun, "Deep residual learning for image recognition," in *Proc. IEEE Conf. Comput. Vis. Pattern Recognit. (CVPR)*, Jun. 2016, pp. 770–778, doi: [10.1109/CVPR.2016.90](https://doi.org/10.1109/CVPR.2016.90).
- [31] K. Simonyan and A. Zisserman, "Very deep convolutional networks for large-scale image recognition," 2014, *arXiv:1409.1556*.



**Carlos Iturrino-García** received the B.S. degree in electrical engineering in instrumentation and automatic control and M.S. degree in electrical engineering in signal processing from the University of Puerto Rico, Mayagüez, Puerto Rico, in 2016 and 2019, respectively. He is currently pursuing the Ph.D. degree in electrical systems with the University of Florence, Florence, Italy.

Since 2019, he is a Researcher with the Department of Information Engineering, University of Florence. His research interests include the applications of machine learning and deep learning algorithms for power quality detection and classification in electrical power system.



**Gabriele Patrizi** (Member, IEEE) received the bachelor's degree (*cum laude*) in electronic and telecommunications engineering and the master's degree (*cum laude*) in electronic engineering and the Ph.D. degree in industrial and reliability engineering from the University of Florence, Florence, Italy, in 2015, 2018, and 2022, respectively.

He is currently a Post-Doctoral Research Fellow in the field of Instrumentation and Measurement and Adjunct Lecturer of Electric Measurements with the University of Florence. His research interests include life cycle reliability of complex systems, condition monitoring for fault diagnosis of electronics, safety instrumented systems, data-driven prognostic, and health management.



**Alessandro Bartolini** (Member, IEEE) received the B.S. degree in electronic and telecommunications engineering and the M.S. degree in electronics engineering from the University of Florence, Florence, Italy, in 2015 and 2018, respectively, where he is currently pursuing the Ph.D. degree in smart industry.

He participated to the NATO-funded project G5014 “Holographic and Impulse Subsurface Radar for Landmine and IED Detection.” His research activities focus on hardware and software design of monitoring devices, energy harvesting, and smart power quality meters.



**Lorenzo Ciani** (Senior Member, IEEE) received the M.S. degree in electronic engineering and the Ph.D. degree in industrial and reliability engineering from the University of Florence, Florence, Italy, in 2005 and 2009, respectively.

He is currently an Associate Professor with the Department of Information Engineering, University of Florence. He has authored or coauthored more than 190 peer-reviewed journal and conference papers. His current research interests include system reliability, availability, maintainability and safety, reliability evaluation test and analysis for electronic systems and devices, fault detection and diagnosis, and electrical and electronic instrumentation and measurement.

Dr. Ciani is a member of the IEEE IMS TC-32 Fault Tolerant Measurement Systems. He received the 2015 IEEE I&M Outstanding Young Engineer Award for “his contribution to the advancement of instrumentation and measurement in the field of reliability analysis.” He is an Associate Editor-in-Chief of the IEEE TRANSACTION ON INSTRUMENTATION AND MEASUREMENT and an Associate Editor of IEEE ACCESS.



**Libero Paolucci** received the master's degree in electrical and automation engineering and the Ph.D. in industrial and reliability engineering from the University of Florence, Florence, Italy, 2014 and 2017, respectively.

He is currently a Research Fellow at the Department of Information Engineering, University of Florence. His current research interests deal with power quality disturbances identification and filtering systems and power electronics design.



**Antonio Luchetta** (Member, IEEE) received the M.S. degree in electronic engineering from the University of Florence, Florence, Italy, in 1993.

From 1995 to 2005, he was an Assistant Professor with the Department of Environmental and Physics Engineering, University of Basilicata, Potenza, Italy, and then with the Department of Electronics and Telecommunications, University of Florence, where he is currently an Associate Professor with the Department of Information Engineering. His current research interests include circuit theory neural networks, symbolic analysis, and simulation of analog circuits.



**Francesco Grasso** (Member, IEEE) received the M.S. degree in electronic engineering and the Ph.D. degree in electronic devices and circuits from the University of Florence, Florence, Italy, in 2000 and 2003, respectively.

He is currently an Associate Professor with the Department of Electronics and Telecommunications, University of Florence. Since 2015, he has been Scientific Director with the Smart Energy Lab, Toolebewong, VIC, Australia, a joint laboratory at the University of Florence on the topics of Power Quality and Smart Grids. Since 2019, he is Innovation Manager for Industry 4.0 at the Ministry of Economic Development and President of UNAE—Institute for Qualification of Plant Installers. His research interests are in the areas of circuit theory, neural networks, and fault diagnosis of electronic.